iScience

CellPress

Article

The Mechanosensitive Ion Channel Piezo1 Significantly Mediates *In Vitro* Ultrasonic Stimulation of Neurons

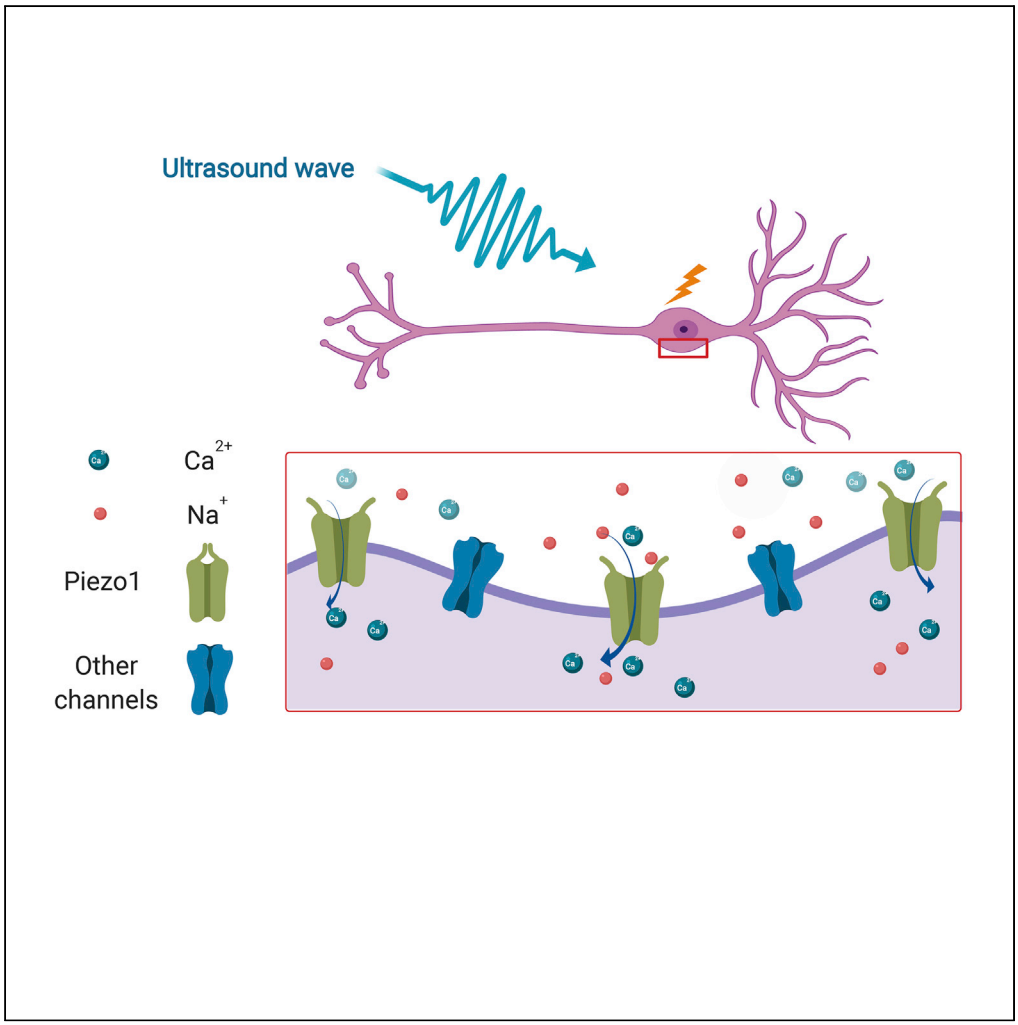

Zhihai Qiu, Jinghui Guo, Shashwati Kala, ..., Hsiao Chang Chan, Hairong Zheng, Lei Sun

hr.zheng@siat.ac.cn (H.Z.)
lei.sun@polyu.edu.hk (L.S.)

HIGHLIGHTS

Piezo1 expressed in HEK293T cells can be activated by low-intensity ultrasound

Ultrasound activates Piezo1 in neurons, increasing Ca^{2+} influx and c-Fos levels

Ca^{2+} influx and signaling triggered by ultrasound depend on acoustic pressure

Piezo1 activation by ultrasound also triggers downstream Ca^{2+} pathway signaling

Qiu et al., iScience *21*, 448–457
November 22, 2019 © 2019 The Author(s).
https://doi.org/10.1016/j.isci.2019.10.037

iScience

CellPress

Article

The Mechanosensitive Ion Channel Piezo1 Significantly Mediates *In Vitro* Ultrasonic Stimulation of Neurons

Zhihai Qiu,[1,4] Jinghui Guo,[1,3,4] Shashwati Kala,[1,4] Jiejun Zhu,[1,4] Quanxiang Xian,[1] Weibao Qiu,[2] Guofeng Li,[2] Ting Zhu,[1] Long Meng,[2] Rui Zhang,[1] Hsiao Chang Chan,[3] Hairong Zheng,[2,*] and Lei Sun[1,5,*]

SUMMARY

Ultrasound brain stimulation is a promising modality for probing brain function and treating brain disease non-invasively and with high spatiotemporal resolution. However, the mechanism underlying its effects remains unclear. Here, we examine the role that the mouse piezo-type mechanosensitive ion channel component 1 (Piezo1) plays in mediating the *in vitro* effects of ultrasound in mouse primary cortical neurons and a neuronal cell line. We show that ultrasound alone could activate heterologous and endogenous Piezo1, initiating calcium influx and increased nuclear c-Fos expression in primary neurons but not when pre-treated with a Piezo1 inhibitor. We also found that ultrasound significantly increased the expression of the important proteins phospho-CaMKII, phospho-CREB, and c-Fos in a neuronal cell line, but Piezo1 knockdown significantly reduced this effect. Our findings demonstrate that the activity of mechanosensitive ion channels such as Piezo1 stimulated by ultrasound is an important contributor to its ability to stimulate cells *in vitro*.

INTRODUCTION

Neuromodulation technologies developed recently, such as magnetic, electric, and optogenetic stimulation methods, have provided unprecedented ways to study brain function and treat its diseases and conditions. Ultrasound is another modality being studied for its neuro-stimulation abilities. Ultrasound beams can be focused on millimeter-sized areas in sub-cortical regions through the intact skull (King et al., 2013; Legon et al., 2014; Tufail et al., 2010). It has been demonstrated to be capable of generating neural responses from the human visual cortex (Lee et al., 2016), somatosensory cortex (Lee et al., 2015; Legon et al., 2014), motor cortex (Legon et al., 2018b), and even the thalamus (Legon et al., 2018a) without obvious side effects. These features have spurred research into ultrasonic neuromodulation, with attempts being made to use it therapeutically for conditions such as Parkinson disease, epilepsy, and depression (Leinenga et al., 2016).

The observed effects of ultrasound, a physical stimulus, in the brain points to central nervous system cells possessing mechanosensitivity by various mechanisms (reviewed by Tyler (2012)). At the low intensities required to apply ultrasound in the brain through the intact skull safely and successfully (Duck, 2007; Fry and Goss, 1980; Tyler et al., 2008), the thermal and cavitation effects of ultrasound are likely to be minor (Dinno et al., 1989; Kim et al., 2014; Tyler et al., 2018). Another possible mechanism of ultrasound is through its action on mechanoresponsive components of cellular machinery, which sense physical forces and initiate cellular signaling. Given the observed timescale of ultrasound's stimulation effects, a plausible explanation is offered by the activity of mechanosensitive ion channels (Bystritsky et al., 2011; Fomenko et al., 2018; Tyler et al., 2018). Such channels are implicated in sensing a wide variety of physical stimuli, including sound, membrane stretch, and shear forces (Martinac, 2012). Some mechanosensitive ion channels have been shown to be activated by ultrasound, but these studies lack the context of brain stimulation, studying either non-mammalian channels (Ibsen et al., 2015; Kubanek et al., 2018; Ye et al., 2018) or mammalian channels expressed in non-neuronal cells (Kubanek et al., 2016).

Among the possible ultrasound-responsive mechanosensitive ion channels, members of the Piezo family are eminent candidates (Coste et al., 2010). The Piezos are very large, evolutionarily conserved transmembrane proteins, and Piezo1 is among the channels most sensitive to physical force (Cox et al., 2017). It can activate and deactivate in the range of milliseconds (Coste et al., 2010) to forces estimated to be as low as

[1]Department of Biomedical Engineering, The Hong Kong Polytechnic University, Hong Kong SAR 999077, P. R. China

[2]Paul C. Lauterbur Research Center for Biomedical Imaging, Institute of Biomedical and Health Engineering, Shenzhen Institutes of Advanced Technology, Chinese Academy of Sciences, Shenzhen, P. R. China

[3]Department of Physiology, School of Medicine, Jinan University, Guangzhou, China

[4]These authors contributed equally

[5]Lead Contact

*Correspondence: hr.zheng@siat.ac.cn (H.Z.), lei.sun@polyu.edu.hk (L.S.)

https://doi.org/10.1016/j.isci.2019.10.037

This is an open access article under the CC BY-NC-ND license (http://creativecommons.org/licenses/by-nc-nd/4.0/).

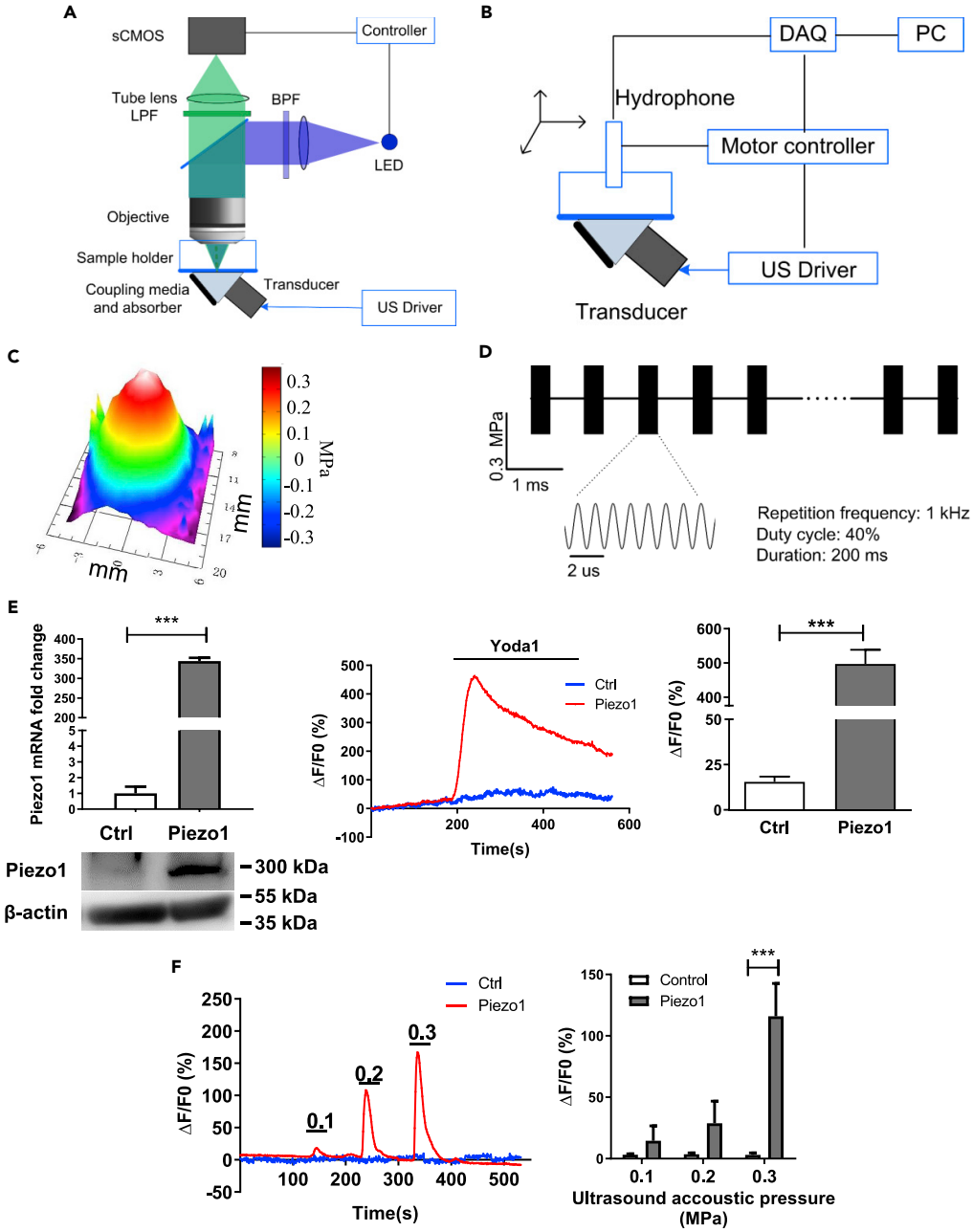

Figure 1. The Mouse Piezo1 Channel Transfected into HEK293T Cells Is Activated by Ultrasound, Using Our Ultrasound Stimulation System

(A) A schematic illustration of our combined calcium imaging and ultrasound system.

(B) A schematic illustration of how the acoustic map of our customized ultrasound system was generated.

(C) Acoustic mapping profile of the controllable ultrasound field generated using the customized setup.

(D) A schematic illustration of the ultrasound stimulation parameters used in our experiments, with a peak-to-peak acoustic pressure of 0.3 MPa used as an example.

(E) The expression of functional mouse Piezo1 in Piezo1-transfected cells ("Piezo1"), compared with a vector control ("Ctrl"), was verified in three ways. Left: qRT-PCR was performed for mouse Piezo1, normalized to β-actin and expressed as a fold change. Bar charts represent the mean ± SEM of three independent experiments. $n = 3$, ***$p < 0.0001$, unpaired two-tailed t test. A representative Western blot of the two groups is also shown. Piezo1 functionality was verified by stimulating cells with 1 μM Piezo1 agonist Yoda1 and performing calcium imaging with Cal-590. Middle: a representative time course of Yoda1 stimulation on the two groups is shown. Right: bar chart shows the mean ± SEM of three independent Ca^{2+} imaging experiments. $n = 10$, ***$p < 0.0001$, unpaired two-tailed t test.

Figure 1. *Continued*

(F) Left: a representative time course of Ca^{2+} imaging comparing ultrasound stimulation at different intensities (numbers represent MPa) of Piezo1-transfected cells compared with the control. Right: the bar chart shows the mean ± SEM of three independent Ca^{2+} imaging experiments. $n = 9$, ***$p < 0.0001$, two-tailed unpaired *t* test with Holm-Sidak correction. All statistically significant differences are shown.

See also Figure S1.

10 pN (Wu et al., 2016). Although it allows cations to permeate cells in general, it is reported to exhibit a preference for calcium ions (Ca^{2+} (Coste et al., 2010). Heterologously expressed Piezo1 could be activated by ultrasound in non-neuronal cells (Gao et al., 2017; Pan et al., 2018; Prieto et al., 2018) but only with the use of very high frequencies or with microbubbles. It remains to be shown whether endogenous Piezo1 in neurons can be activated by ultrasound alone and what role this interaction could play in neuro-stimulation by ultrasound.

In the present study we confirm endogenous Piezo1 expression in mouse primary neurons, and in a neuronal cell line, and show that these channels play a role in neuronal activation *in vitro*. We demonstrate that low-intensity low-frequency ultrasound alone can activate heterologously expressed HEK293T cells, as well as endogenous Piezo1 channels, initiating Ca^{2+} influx and increasing levels of c-Fos. We also show ultrasound is capable of significantly affecting the levels of downstream Ca^{2+} signaling proteins crucially involved in neuronal function and that knocking down Piezo1 significantly decreased this effect. Thus, we show that Piezo1 activation plays a major role in the mechanotransduction of ultrasound and that ultrasound alone is capable of significantly affecting the function and activation of neurons *in vitro*.

RESULTS

Customized *In Vitro* Ultrasound Stimulation Setup

We developed a customized *in vitro* ultrasound stimulation system incorporated with a calcium imaging system (Figure 1A). Briefly, the calcium imaging system consisted of a modified upright epifluorescence microscope. The excitation light was generated by a dual-color LED, filtered and delivered to the sample to illuminate the calcium sensor. Signals from the cells were collected by a water immersion objective, passed through a dual-filter wheel, and captured by a camera. To minimize phototoxic effects, the LEDs were triggered at 1 Hz and synchronized with sCMOS time-lapse imaging. Ultrasound was delivered through a triangle waveguide attached to the transducer placed below the culture dish at a 45-degree angle. The waveguide was also attached to an acoustic absorber to minimize acoustic reverberation. This design helped us to minimize the generation of standing waves and created a strong water-air interface on the bottom of the dish. This results in a controllable ultrasound field, as measured by an acoustic pressure mapping system consisting of a needle hydrophone and high-precision 3D motor (Figure 1B). The obtained acoustic pressure map is displayed in Figure 1C, using an acoustic pressure of 0.3 MPa for illustration. Each stimulus was composed of 200 tone burst pulses at a center frequency of 500 kHz with a duty cycle of 40% at a pulse repetition frequency (PRF) of 1 kHz, at low acoustic intensities (Figure 1D). These parameters corresponded to very short bursts of ultrasound stimulation, helping to minimize any resultant thermal effects (Kubanek et al., 2018).

Heterologously Expressed Piezo1 Can Be Activated by Ultrasound and Induce Ca^{2+} Influx in HEK293T Cells

To confirm that ultrasound could activate Piezo1 using our customized setup, we overexpressed mouse Piezo1 heterologously in HEK293T cells, known to show minimal response to mechanical stimulation (Coste et al., 2010; Syeda et al., 2015). We transfected cells with a pcDNA3.1-mPiezo1-IRES-GFP plasmid (described in Coste et al. (2010)) or a vector control (described in Schaefer et al. (2008)) and treated them with a Piezo1-specific agonist, Yoda1 (Syeda et al., 2015). We verified the overexpression using qRT-PCT and Western blotting for Piezo1, and calcium imaging revealed that 1 μM Yoda1 induced significantly more Ca^{2+} influx in the Piezo1-transfected cells, compared with the control (Figure 1E). We thus confirmed the expression and functionality of transfected mouse Piezo1 channels in HEK293T cells.

We proceeded to perform Ca^{2+} using ultrasound at acoustic pressures corresponding to a range previously reported to have elicited responses (Tufail et al., 2010). We found that increasing ultrasound pressure on Piezo1-transfected cells resulted in increasing Ca^{2+} influx into cells, with 0.3 MPa ultrasound showing a significant increase, whereas the control remained largely unchanged (Figure 1E). To exclude the possibility

that the fluorescence changes were due to cells being out-of-focus due to ultrasound perturbation, we also performed ratiometric Ca^{2+} imaging. We observed that the fluorescence ratio (340/380) of control cells showed no response, whereas the Piezo1-expressing cells showed a robust and large response to 0.1 MPa ultrasound (Figure S1). Pre-treating the Piezo1-expressing cells with a Piezo1-specific inhibitor, GsMTx-4 (Bae et al., 2011), at 40 μM reduced the cells' response to the same level as the control cells (Figure S1). This finding confirmed that the elevated cytoplasmic Ca^{2+} levels seen upon ultrasound stimulation were not experimental artifacts. Thus, our ultrasound stimulation setup could successfully activate Piezo1 to allow Ca^{2+} influx at low, physiologically relevant acoustic pressures.

Mouse Primary Neurons Are Activated by Ultrasound in a Piezo1 Activity-Dependent Manner

We next tested the effects of ultrasound on primary cortical neurons harvested from embryonic mice to test the feasibility of stimulating live neurons with ultrasound. We first probed whether primary neurons cultured using our protocol could express any functional Piezo1. Treating primary neurons at DIV 10 with 10 μM Yoda1 stimulated Ca^{2+} influx, whereas pre-treatment with 40 μM GsMTx-4 significantly reduced it (Figure 2A). The inhibitory effect of GsMTx-4 upon Yoda1-induced Ca^{2+} influx was consistent with the known mechanism of its action as a Piezo1 gating modifier (Bae et al., 2011; Gnanasambandam et al., 2017). Immunofluorescent staining revealed that primary neurons at day *in vitro* (DIV) 10 expressed Piezo1 endogenously (Figure 2B). Thus, primary neurons at DIV 10 expressed some functional Piezo1, and we proceeded to evaluate the effects of ultrasound on these cells. We also acutely isolated mouse cortical neurons from mouse pups at P3, to evaluate *in vivo* expression of Piezo1 in neurons of approximately equal maturity. These neurons influxed Ca^{2+} when stimulated with Yoda1, but this effect was almost completely abrogated in presence of the mechanosensitive ion channel antagonist Ruthenium red (Figure S2). We thus found that mature neurons, both *in vitro* and *in vivo*, expressed functional Piezo1 with detectable effects.

Ultrasound stimulation resulted in dose-dependent Ca^{2+} influx into the neurons, and this influx was abrogated when the cells were pre-treated with 40 μM GsMTx-4 (Figure 2C). Ultrasound at 0.3 MPa and above was able to induce significant Ca^{2+} influx, so we evaluated the effects of ultrasound on neuron activation by immunofluorescent staining of c-Fos, a well-established molecular marker of neuronal activation that is responsive to Ca^{2+} influx (Chaudhuri et al., 2000; Ghosh et al., 1994; Sheng and Greenberg, 1990). Untreated cells, cells treated with 0.3 MPa ultrasound for 20 min and cells pre-treated with 20 μM GsMTx-4 before ultrasound inside a standard cell culture incubator (setup illustrated in Figure 2D), were compared. We found that c-Fos expression in the nuclei of neurons (identified by MAP2 staining) significantly increased upon US treatment compared with the untreated control and reduced significantly with GsMTx-4 pre-treatment (Figure 2E). Hence, low-intensity ultrasound could activate primary neurons *in vitro* by opening the Piezo1 channel to allow Ca^{2+} influx.

Ultrasound Requires Piezo1 to Induce Calcium-Dependent Downstream Signaling in a Neuronal Cell Line

We were interested in exploring the signaling implications of Piezo1-mediated ultrasound effects on neurons in greater depth, to help elucidate the possible downstream effects of Ca^{2+} influx through ultrasound-activated Piezo1 channels. We chose the mouse hippocampal cell line mHippoE-18 (CLU199) as an *in vitro* representation of normal (non-cancerous) neuronal cells to enable better quantification of these effects. Expression of Piezo1 in CLU199 cells was confirmed through semi-quantitative RT-PCR, with HeLa cells as a positive control (McHugh et al., 2010) and Western blot (Figure 3A). To evaluate the treatment's effects on cell signaling downstream of the observed Ca^{2+} influx, we investigated levels of the phosphorylated (activated) forms of the Ca^{2+}/calmodulin-dependent protein kinase type II (p-CaMKII) and the transcription factor CREB (p-CREB). Both these proteins are crucial players in neuronal Ca^{2+} signaling. CaMKII is directly regulated by calmodulin, a good indicator of the level of Ca^{2+} inside the cell, and both CaMKII and CREB are involved in critical neuronal functions such as neurotransmitter secretion, plasticity, transcription regulation, learning, and memory (Hardingham et al., 2001; Yamauchi, 2005). We observed the levels of these activated proteins, along with c-Fos, by Western blot to gauge whether ultrasound could affect aspects of neuronal function and activation downstream of Ca^{2+} influx. Ultrasound treatment inside an incubator for 20 min increased the levels of p-CaMKII, p-CREB, and c-Fos in a dose-dependent manner, with 0.3 and 0.5 MPa inducing significant increases (Figure 3B). We then evaluated Piezo1's contribution to these effects by siRNA knockdown. We were able to achieve over 50% knockdown of Piezo1 and found that this significantly reduced the 1 μM Yoda1-induced Ca^{2+} influx compared with cells treated with non-targeting siRNA ("Ctrl") (Figure 3C). CLU199 cells with Piezo1 knockdown also displayed no significant upregulation of p-CaMKII,

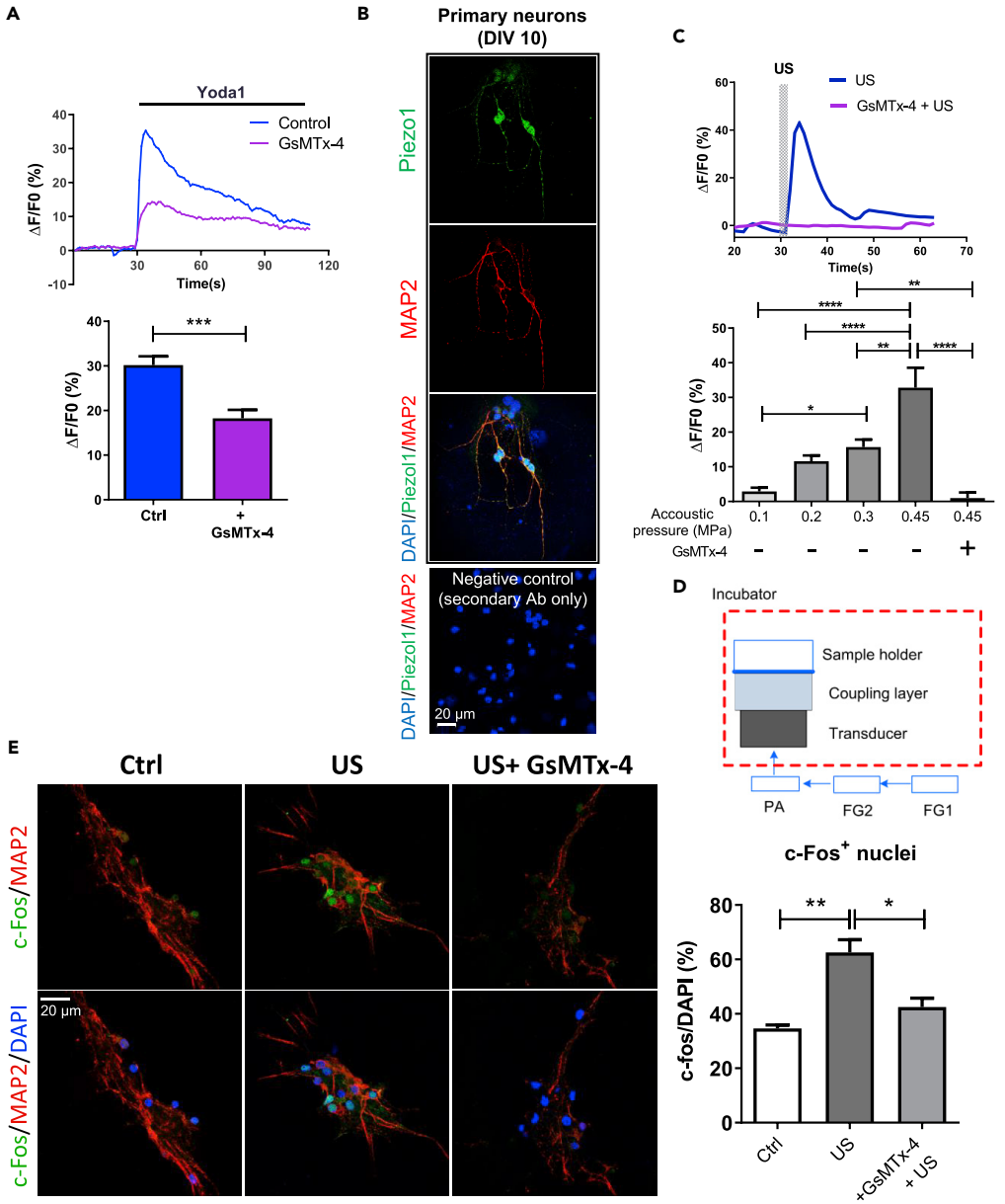

Figure 2. Ultrasound Induces Ca^{2+} Influx and c-Fos Expression in Primary Neurons in a Piezo1 Activity-Dependent Manner

(A) Functionality of Piezo1 in primary neurons was examined by Ca^{2+} imaging of cells stimulated with Piezo1 agonist Yoda1, including cells pre-treated with Piezo1 blocker GsMTx-4. Top: representative Ca^{2+} imaging time course for cells treated with either 10 μM Yoda1 alone or pre-treated with 40 μM GsMTx-4, respectively. Bar chart shows the mean ± SEM of three independent experiments. $n = 15$, ***$p < 0.001$, unpaired two-tailed t test.

(B) Piezo1 expression in primary cortical neurons was examined by immunocytochemical staining. Representative images of Piezo1 and MAP2 immunocytochemical staining of mouse primary cortical neurons at DIV 10.

(C) Ca^{2+} imaging of primary neurons stimulated with ultrasound, including cells pre-treated with GsMTx-4. Top: representative Ca^{2+} imaging time course of primary neurons treated with 0.45 MPa ultrasound or pre-treated with 40 μM GsMTx-4 and then with ultrasound. Bottom: bar chart represents mean ± SEM of three independent experiments treating primary neurons with varying intensities of ultrasound and GsMTx-4. $n = 9$, *$p < 0.05$, **$p < 0.01$, ***$p < 0.001$, one-way ANOVA with post-hoc Tukey test. All statistically significant differences are shown. See also Figure S2.

(D) An illustration of the ultrasound setup used to treat cells placed inside a cell culture incubator for immunofluorescence or Western blots.

(E) Left: representative IF images of c-Fos and MAP2 staining, in cells that were untreated, treated with 0.3 MPa ultrasound, or with 20 μM GsMTx-4 followed by ultrasound. Right: bar chart represents the mean ± SEM of three independent experiments. $n = 3$, *$p < 0.05$, **$p < 0.01$, one-way ANOVA with post-hoc Tukey test.

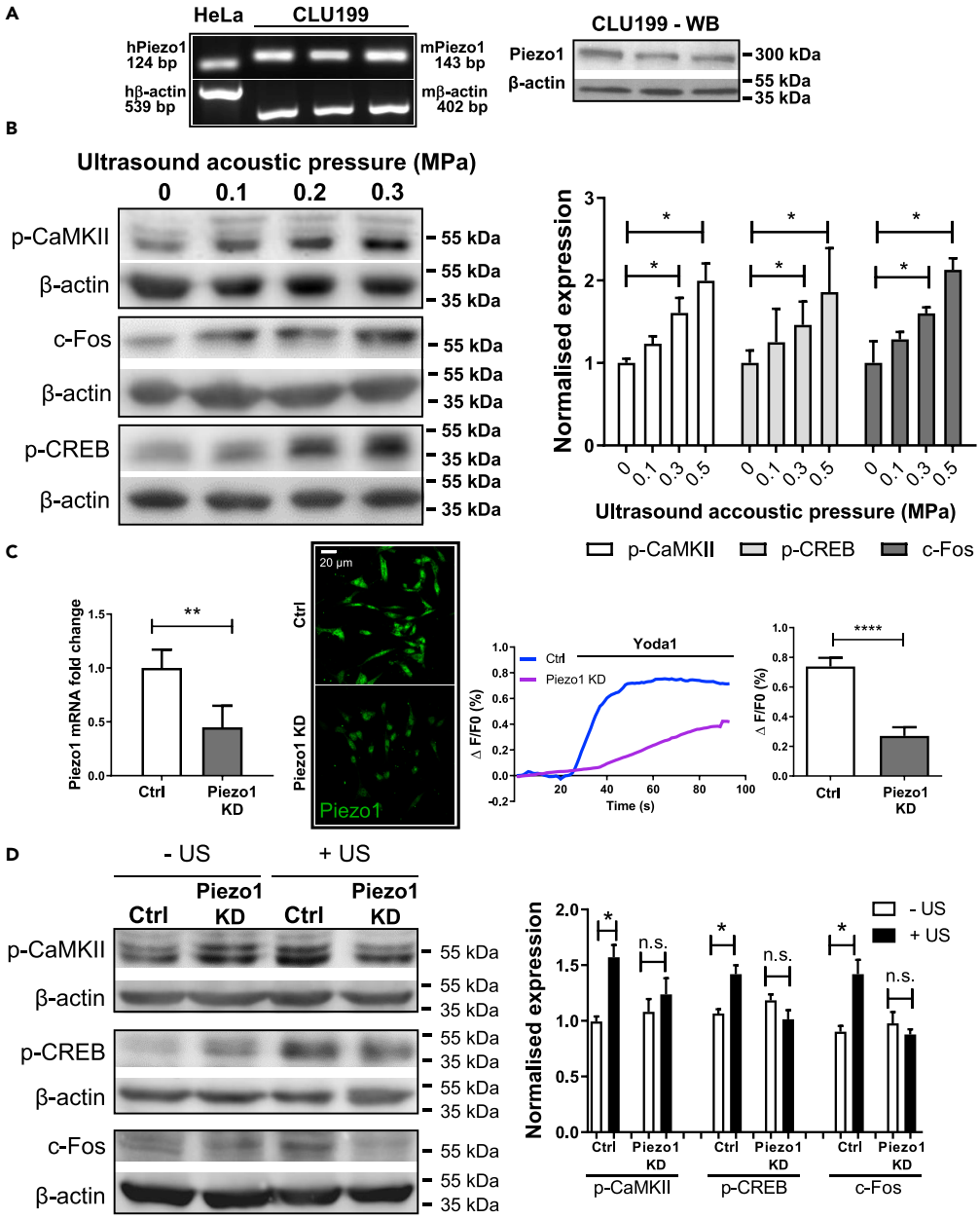

Figure 3. Ultrasound's Ability to Initiate Calcium-Dependent Downstream Signaling in CLU199 Cells Is Dependent on Piezo1

(A) Levels of Piezo1 in a mouse neuronal cell line, CLU199, were evaluated in two ways. Left: PCR results of Piezo1 expression in multiple samples of CLU199 cells, with HeLa cells for comparison. Right: Western blot of Piezo1 expression in multiple samples of CLU199.

(B) Western blot for expression levels of p-CaMKII, p-CREB, and c-Fos, in CLU199 cells treated with varying ultrasound intensities. Left: representative Western blot images. Right: bar chart shows the levels of each protein as a fold change compared with the untreated control. Results are mean ± SEM of three independent experiments. $n = 3$, *$p < 0.05$, unpaired two-tailed t test.

(C) Piezo1 was knocked down in CLU199 cell using non-targeting ('Ctrl') or Piezo1 siRNA ("Piezo1 KD"). Left: qRT-PCR was performed for Piezo1, normalized to β-actin, and expressed as a fold change. Bar chart represents mean ± SEM of three independent experiments. $n = 3$, **$p < 0.01$, unpaired two-tailed t test. Also shown are representative IF images of Piezo1 staining in CLU199 cells. Middle: representative Ca^{2+} imaging time course for Ctrl and Piezo1 KD cells treated with Yoda1. Right: bar chart shows the mean ± SEM of three independent Ca^{2+} imaging experiments. $n = 13$, ***$p < 0.001$, unpaired two-tailed t test with Holm-Sidak correction.

Figure 3. *Continued*
(D) Western blot for levels of p-CaMKII, p-CREB, and c-Fos in CLU199 cells treated with siRNA and ultrasound. Left: representative Western blot images. Right: bar chart shows the levels of each protein as a fold change compared with the untreated control. Results are mean ± SEM of three independent experiments. $n = 3$, *$p < 0.05$, unpaired two-way ANOVA with post-hoc Tukey test.

p-CREB, and c-Fos than the control when treated with 0.3 MPa ultrasound compared with the control (Figure 3D). Thus, we determined that ultrasound stimulation significantly affects the levels of important proteins in CLU199 neuronal cells, and these effects were significantly mediated by the Piezo1 channel.

DISCUSSION

In the present study, we show that Piezo1 expressed in neurons is an important mediator of ultrasound's *in vitro* effects. We observed that heterologous Piezo1 expression in cells could enable them to respond to ultrasound (HEK293T). We showed that mouse neuronal cells express Piezo1 endogenously and that ultrasound alone can open these channels, allowing Ca^{2+} influx into them. We also demonstrated that activation of primary neurons by ultrasound *in vitro* can be significantly reduced by inhibiting Piezo1's activity. Our experiments used low-intensity low-frequency ultrasound, without microbubbles, allowing us to minimize the thermal and cavitation effects of ultrasound. We manipulated endogenous Piezo1 on a functional level, using an inhibitor drug, and at the expression level, using siRNA, and found that the effects of ultrasound on proteins crucially involved in neuronal activation and calcium signaling were significantly reduced in both cases. Blocking the activity of heterologous Piezo1 could also suppress ultrasound-induced Ca^{2+} influx. Thus, we see an important role played by Piezo1 activation in enabling neurons to respond to ultrasound stimulation.

In addition to increased c-Fos expression in primary neurons, our results in a neuronal cell line also showed that the expression of the activated forms of CaMKII and CREB can be increased by ultrasound stimulation, along with increasing c-Fos expression. These proteins are involved in complex neuronal functions such as neuronal plasticity, learning, and memory. Although results from a cell line must not be overinterpreted, previous studies of ultrasound have also shown increases of calmodulin-dependent kinases in primary neurons (Liu et al., 2017) and increases in the crucial neuroprotective protein BDNF in mouse and rat brains treated with ultrasound (Chen et al., 2018; Su et al., 2017; Tufail et al., 2010). The observed Piezo1-dependence of these effects in our experiments also helps to pinpoint their source to the ultrasound stimulation. Such results at the cellular level also provide evidence of the basis for non-auditory effects of ultrasound. Our results help to bolster the idea that ultrasound treatment can have therapeutic effects in the brain and could contribute to identifying which conditions could benefit most from such a treatment.

The obvious next step would be to demonstrate Piezo1-dependence of ultrasound effects *in vivo*, by upregulating or downregulating it in rodent brains. It will likely be challenging to upregulate Piezo1 *in vivo*, due to its size and complexity (Coste et al., 2010, 2015), but also to downregulate it, as knocking it out totally in mice embryos can be lethal (Li et al., 2015; Ranade et al., 2014). However, delivering a Piezo1 inhibitor or Piezo1 knockdown reagents in rodents is feasible and is a promising approach for further understanding the effects of ultrasound. Transgenic mice with conditional knockout of Piezo1 in the brain are also a viable option. Concurrently, research about the Piezo1 molecule itself could contribute to both evaluating and enhancing the role of brain-based Piezo1 in mediating ultrasound's effects. Studies comparing the different segments show some domains to be more mechanosensitive than other (Wu et al., 2016). This raises the possibility that the effects of ultrasound on such domains could be studied instead of the entire molecule, making it easier to tailor ultrasound parameters to activate Piezo1 more efficiently. Knowledge of this kind could also have significance in other fields, as Piezo1 plays crucial roles in other systems, such as the development of blood vessels (Li et al., 2015; Ranade et al., 2014) or T-cell activation (Liu et al., 2018). Thus, understanding ultrasound's mechanism of action on Piezo1 could have implications for usefully modulating neuronal activity, as well as that of a host of other cell types.

Limitations of the Study

Although we aimed to demonstrate that ultrasound opens the Piezo1 channel, we could not use the standard method of patch clamping to determine this. This is because the recording pipette in our system was found to be incompatible with low-frequency ultrasound, a phenomenon also reported elsewhere (Prieto et al., 2018). We thus used intracellular ratiometric Ca^{2+} imaging to measure the ion influx resulting from ultrasound opening Piezo1, which helped us work around the vibration issue. It is also important to note

that the cells used in this study were cultured on lysine-coated glass, a hard substrate, as this can complicate data interpretation. Ultrasound could cause vibrations in the base of the dish, amplifying the observed effects (Kubanek et al., 2016), leading to an underestimation of the acoustic pressure required to activate Piezo1. Secondly, neurons develop divergently depending upon the stiffness of their surroundings (Chang et al., 2017; Koser et al., 2016), and substrate stiffness is also reported to affect Piezo1's activity (Pathak et al., 2014). A possible solution would be to coat plates with a soft gel that mimics the mechanical properties of brain tissue. However, there is no standard method to achieve this, which is why we opted to maintain a simple culture protocol to avoid unnecessary complications. An aim of future studies ought to be to solve such issues *in vitro*, to gain more physiologically relevant data.

Finally, we did not examine the role of other mechanosensitive ion channels that may be involved in mediating the cellular response to ultrasound, because we were primarily interested in whether low-intensity ultrasound stimulation could activate our chosen Piezo1 channel. For all three issues, in the context of the present study, we based our conclusions upon comparison to controls, with lower Piezo1 expression or with a Piezo1 blocker, which were also exposed to ultrasound but showed significantly lower (but not abrogated) responses. We thus argue that Piezo1 mediated ultrasound's effects in our cells to a considerable degree, a finding that could be adapted and applied to *in vivo* conditions as appropriate. However, future studies with *in vivo* Piezo1 knockout/knockdown in brains and using sensitive genetically encoded Ca^{2+} or voltage sensors for real-time tracking of ultrasound's effects will be crucial to truly establish the role of channels as Piezo1 in this context.

METHODS

All methods can be found in the accompanying Transparent Methods supplemental file.

DATA AND CODE AVAILABILITY

The authors confirm that the data supporting the findings of this study are available within the article and its Supplemental Information.

SUPPLEMENTAL INFORMATION

Supplemental Information can be found online at https://doi.org/10.1016/j.isci.2019.10.037.

ACKNOWLEDGMENTS

We thank Dr. Ardem Patapoutian and Dr. Kathleen L Collins for providing the Piezo1 and control plasmids used in this study. This work was supported by the Hong Kong Research Grants Council General Research Fund (15102417 and 15326416), Shenzhen Basic Research Funding Scheme (JCYJ20160531184809079), National Research Instrumental Development Fund of the National Science Foundation of China (81527901), and internal funding from The Hong Kong Polytechnic University (1-YW0Q, 1-ZVGK, 4-BBAU, and G-YZ1N).

AUTHOR CONTRIBUTIONS

S. K., Z. Q., J. G., and L. S. drafted the manuscript. S.K., J. G., J. Z., and H. C. C. designed the cellular experiments. Z. Q., W. Q., L. M., H. Z., and L. S. designed the ultrasound stimulation instrument and experiments. S.K. cultured HEK293T and CLU199 cells and performed transfections. Q. X., R. Z., and T. Z. harvested and cultured primary neurons. Z. Q. and J. G. performed calcium imaging and analysis. S. K. conducted IF, WB, and RT-PCR and analyzed the resultant data. Z. Q. and L. S. originally conceived the selective ultrasound stimulation concept.

DECLARATION OF INTERESTS

Z.Q., J.G., S.K., J. Z., Q. Z., and L.S. have submitted a patent application titled "A Non-invasive method for selective neural stimulation by ultrasound" with the USPTO dated April 10, 2018, assigned application number 15/949,991, which relates to the ultrasound setup used in all the experiments. The authors declare no further financial interests.

Received: May 3, 2019
Revised: September 4, 2019
Accepted: October 18, 2019
Published: November 22, 2019

REFERENCES

Bae, C., Sachs, F., and Gottlieb, P.A. (2011). The mechanosensitive ion channel piezo1 is inhibited by the peptide GsMTx4. Biochemistry *50*, 6295–6300.

Bystritsky, A., Korb, A.S., Douglas, P.K., Cohen, M.S., Melega, W.P., Mulgaonkar, A.P., DeSalles, A., Min, B.K., and Yoo, S.S. (2011). A review of low-intensity focused ultrasound pulsation. Brain Stimul. *4*, 125–136.

Chang, T.Y., Chen, C., Lee, M., Chang, Y.C., Lu, C.H., Lu, S.T., Wang, D.Y., Wang, A., Guo, C.L., and Cheng, P.L. (2017). Paxillin facilitates timely neurite initiation on soft-substrate environments by interacting with the endocytic machinery. Elife *6*, e31101, https://doi.org/10.7554/eLife.31101.

Chaudhuri, A., Zangenehpour, S., Rahbar-Dehgan, F., and Ye, F. (2000). Molecular maps of neural activity and quiescence. Acta Neurobiol. Exp. (Wars) *60*, 403–410.

Chen, C.M., Wu, C.T., Yang, T.H., Liu, S.H., and Yang, F.Y. (2018). Preventive effect of low intensity pulsed ultrasound against experimental cerebral ischemia/reperfusion injury via apoptosis reduction and brain-derived neurotrophic factor induction. Sci. Rep. *8*, 5568.

Coste, B., Mathur, J., Schmidt, M., Earley, T.J., Ranade, S., Petrus, M.J., Dubin, A.E., and Patapoutian, A. (2010). Piezo1 and Piezo2 are essential components of distinct mechanically activated cation channels. Science *330*, 55–60.

Coste, B., Murthy, S.E., Mathur, J., Schmidt, M., Mechioukhi, Y., Delmas, P., and Patapoutian, A. (2015). Piezo1 ion channel pore properties are dictated by C-terminal region. Nat. Commun. *6*, 7223.

Cox, C.D., Bavi, N., and Martinac, B. (2017). Origin of the force: the force-from-lipids principle applied to piezo channels. Curr. Top. Membr. *79*, 59–96.

Dinno, M.A., Dyson, M., Young, S.R., Mortimer, A.J., Hart, J., and Crum, L.A. (1989). The significance of membrane-changes in the safe and effective use of therapeutic and diagnostic ultrasound. Phys. Med. Biol. *34*, 1543–1552.

Duck, F.A. (2007). Medical and non-medical protection standards for ultrasound and infrasound. Prog. Biophys. Mol. Biol. *93*, 176–191.

Fomenko, A., Neudorfer, C., Dallapiazza, R.F., Kalia, S.K., and Lozano, A.M. (2018). Low-intensity ultrasound neuromodulation: an overview of mechanisms and emerging human applications. Brain Stimul. *11*, 1209–1217.

Fry, F.J., and Goss, S.A. (1980). Further-studies of the transkull transmission of an intense focused ultrasonic beam - lesion production at 500 Khz. Ultrasound Med. Biol. *6*, 33–38.

Gao, Q.H., Cooper, P.R., Walmsley, A.D., and Scheven, B.A. (2017). Role of piezo channels in ultrasound-stimulated dental stem cells. J. Endod. *43*, 1130–1136.

Ghosh, A., Ginty, D.D., Bading, H., and Greenberg, M.E. (1994). Calcium regulation of gene expression in neuronal cells. J. Neurobiol. *25*, 294–303.

Gnanasambandam, R., Ghatak, C., Yasmann, A., Nishizawa, K., Sachs, F., Ladokhin, A.S., Sukharev, S.I., and Suchyna, T.M. (2017). GsMTx4: mechanism of inhibiting mechanosensitive ion channels. Biophys. J. *112*, 31–45.

Hardingham, G.E., Arnold, F.J., and Bading, H. (2001). Nuclear calcium signaling controls CREB-mediated gene expression triggered by synaptic activity. Nat. Neurosci. *4*, 261–267.

Ibsen, S., Tong, A., Schutt, C., Esener, S., and Chalasani, S.H. (2015). Sonogenetics is a non-invasive approach to activating neurons in Caenorhabditis elegans. Nat. Commun. *6*, 8264.

Kim, H., Chiu, A., Lee, S.D., Fischer, K., and Yoo, S.S. (2014). Focused ultrasound-mediated non-invasive brain stimulation: examination of sonication parameters. Brain Stimul. *7*, 748–756.

King, R.L., Brown, J.R., Newsome, W.T., and Pauly, K.B. (2013). Effective parameters for ultrasound-induced in vivo neurostimulation. Ultrasound Med. Biol. *39*, 312–331.

Koser, D.E., Thompson, A.J., Foster, S.K., Dwivedy, A., Pillai, E.K., Sheridan, G.K., Svoboda, H., Viana, M., Costa, L.D., Guck, J., et al. (2016). Mechanosensing is critical for axon growth in the developing brain. Nat. Neurosci. *19*, 1592–1598.

Kubanek, J., Shi, J., Marsh, J., Chen, D., Deng, C., and Cui, J. (2016). Ultrasound modulates ion channel currents. Sci. Rep. *6*, 24170.

Kubanek, J., Shukla, P., Das, A., Baccus, S.A., and Goodman, M.B. (2018). Ultrasound elicits behavioral responses through mechanical effects on neurons and ion channels in a simple nervous system. J. Neurosci. *38*, 3081–3091.

Lee, W., Kim, H., Jung, Y., Song, I.U., Chung, Y.A., and Yoo, S.S. (2015). Image-guided transcranial focused ultrasound stimulates human primary somatosensory cortex. Sci. Rep. *5*, 8743.

Lee, W., Kim, H.C., Jung, Y., Chung, Y.A., Song, I.U., Lee, J.H., and Yoo, S.S. (2016). Transcranial focused ultrasound stimulation of human primary visual cortex. Sci. Rep. *6*, 34026.

Legon, W., Ai, L., Bansal, P., and Mueller, J.K. (2018a). Neuromodulation with single-element transcranial focused ultrasound in human thalamus. Hum. Brain Mapp. *39*, 1995–2006.

Legon, W., Bansal, P., Tyshynsky, R., Ai, L., and Mueller, J.K. (2018b). Transcranial focused ultrasound neuromodulation of the human primary motor cortex. Sci. Rep. *8*, 10007.

Legon, W., Sato, T.F., Opitz, A., Mueller, J., Barbour, A., Williams, A., and Tyler, W.J. (2014). Transcranial focused ultrasound modulates the activity of primary somatosensory cortex in humans. Nat. Neurosci. *17*, 322–329.

Leinenga, G., Langton, C., Nisbet, R., and Gotz, J. (2016). Ultrasound treatment of neurological diseases–current and emerging applications. Nat. Rev. Neurol. *12*, 161–174.

Liu, C.S.C., Raychaudhuri, D., Paul, B., Chakrabarty, Y., Ghosh, A.R., Rahaman, O., Talukdar, A., and Ganguly, D. (2018). Cutting edge: piezo1 mechanosensors optimize human T cell activation. J. Immunol. *200*, 1255–1260.

Li, J., Hou, B., Tumova, S., Muraki, K., Bruns, A., Ludlow, M.J., Sedo, A., Hyman, A.J., McKeown, L., Young, R.S., et al. (2015). Piezo1 integration of vascular architecture with physiological force. FASEB J. *29*, 279, https://doi.org/10.1038/nature13701.

Liu, S.-H., Lai, Y.-L., Chen, B.-L., and Yang, F.-Y. (2017). Ultrasound enhances the expression of brain-derived neurotrophic factor in astrocyte through activation of TrkB-Akt and calcium-CaMK signaling pathways. Cereb. Cortex *27*, 3152–3160.

Martinac, B. (2012). Mechanosensitive ion channels: an evolutionary and scientific tour de force in mechanobiology. Channels (Austin) *6*, 211–213.

McHugh, B.J., Buttery, R., Lad, Y., Banks, S., Haslett, C., and Sethi, T. (2010). Integrin activation by Fam38A uses a novel mechanism of R-Ras targeting to the endoplasmic reticulum. J. Cell Sci. *123*, 51–61.

Pan, Y.J., Yoon, S., Sun, J., Huang, Z.L., Lee, C.Y., Allen, M., Wu, Y.Q., Chang, Y.J., Sadelain, M., Shung, K.K., et al. (2018). Mechanogenetics for the remote and noninvasive control of cancer immunotherapy. Proc. Natl. Acad. Sci. U S A *115*, 992–997.

Pathak, M.M., Nourse, J.L., Tran, T., Hwe, J., Arulmoli, J., Le, D.T., Bernardis, E., Flanagan, L.A., and Tombola, F. (2014). Stretch-activated ion channel Piezo1 directs lineage choice in human neural stem cells. Proc. Natl. Acad. Sci. U S A *111*, 16148–16153.

Prieto, M.L., Firouzi, K., Khuri-Yakub, B.T., and Maduke, M. (2018). Activation of piezo1 but not NaV1.2 channels by ultrasound at 43 MHz. Ultrasound Med. Biol. *44*, 1217–1232.

Ranade, S.S., Qiu, Z.Z., Woo, S.H., Hur, S.S., Murthy, S.E., Cahalan, S.M., Xu, J., Mathur, J., Bandell, M., Coste, B., et al. (2014). Piezo1, a mechanically activated ion channel, is required for vascular development in mice. P Natl. Acad. Sci. USA *111*, 10347–10352.

Schaefer, M.R., Williams, M., Kulpa, D.A., Blakely, P.K., Yaffee, A.Q., and Collins, K.L. (2008). A novel trafficking signal within the HLA-C cytoplasmic tail allows regulated expression upon differentiation of macrophages. J. Immunol. *180*, 7804–7817.

Sheng, M., and Greenberg, M.E. (1990). The regulation and function of c-fos and other immediate early genes in the nervous system. Neuron *4*, 477–485.

Su, W.S., Wu, C.H., Chen, S.F., and Yang, F.Y. (2017). Transcranial ultrasound stimulation promotes brain-derived neurotrophic factor and

reduces apoptosis in a mouse model of traumatic brain injury. Brain Stimul. *10*, 1032–1041.

Syeda, R., Xu, J., Dubin, A.E., Coste, B., Mathur, J., Huynh, T., Matzen, J., Lao, J., Tully, D.C., Engels, I.H., et al. (2015). Chemical activation of the mechanotransduction channel Piezo1. Elife *4*, e07369, https://doi.org/10.7554/eLife.07369.

Tufail, Y., Matyushov, A., Baldwin, N., Tauchmann, M.L., Georges, J., Yoshihiro, A., Tillery, S.I., and Tyler, W.J. (2010). Transcranial pulsed ultrasound stimulates intact brain circuits. Neuron *66*, 681–694.

Tyler, W.J. (2012). The mechanobiology of brain function. Nat. Rev. Neurosci. *13*, 867–878.

Tyler, W.J., Lani, S.W., and Hwang, G.M. (2018). Ultrasonic modulation of neural circuit activity. Curr. Opin. Neurobiol. *50*, 222–231.

Tyler, W.J., Tufail, Y., Finsterwald, M., Tauchmann, M.L., Olson, E.J., and Majestic, C. (2008). Remote excitation of neuronal circuits using low-intensity, low-frequency ultrasound. PLoS One *3*, e3511.

Wu, J., Goyal, R., and Grandl, J. (2016). Localized force application reveals mechanically sensitive domains of Piezo1. Nat. Commun. *7*, 12939.

Yamauchi, T. (2005). Neuronal Ca2+/calmodulin-dependent protein kinase II–discovery, progress in a quarter of a century, and perspective: implication for learning and memory. Biol. Pharm. Bull. *28*, 1342–1354.

Ye, J., Tang, S.Y., Meng, L., Li, X., Wen, X.X., Chen, S.H., Niu, L.L., Li, X.Y., Qiu, W.B., Hu, H.L., et al. (2018). Ultrasonic control of neural activity through activation of the mechanosensitive channel MscL. Nano Lett. *18*, 4148–4155.

ISCI, Volume *21*

Supplemental Information

The Mechanosensitive Ion Channel Piezo1 Significantly Mediates *In Vitro* Ultrasonic Stimulation of Neurons

Zhihai Qiu, Jinghui Guo, Shashwati Kala, Jiejun Zhu, Quanxiang Xian, Weibao Qiu, Guofeng Li, Ting Zhu, Long Meng, Rui Zhang, Hsiao Chang Chan, Hairong Zheng, and Lei Sun

Supplemental Information

Supplemental Figures 1-2

Transparent Methods

Supplemental References

Supplemental Figures

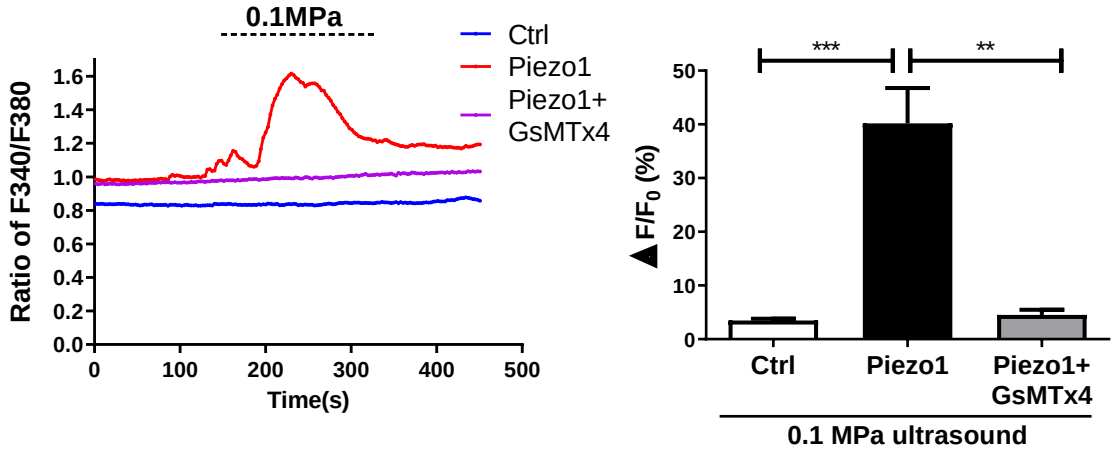

Figure S1. Ratiometric Ca^{2+} imaging of 293T cells treated with ultrasound, related to Figure 1

Ratiometric Ca^{2+} imaging was performed using Fura-2. Left: Representative time-course for vector control plasmid-transfected cells ('Ctrl'), Piezo1-transfected cells ('Piezo1') and Piezo1-transfected cells pre-treated with 40 µM GsMTx-4 , treated with 0.1 MPa ultrasound. Right: Bar charts show the mean ± SEM of 4 independent experiments, *n* = 4, one-way ANOVA with post-hoc Tukey test.

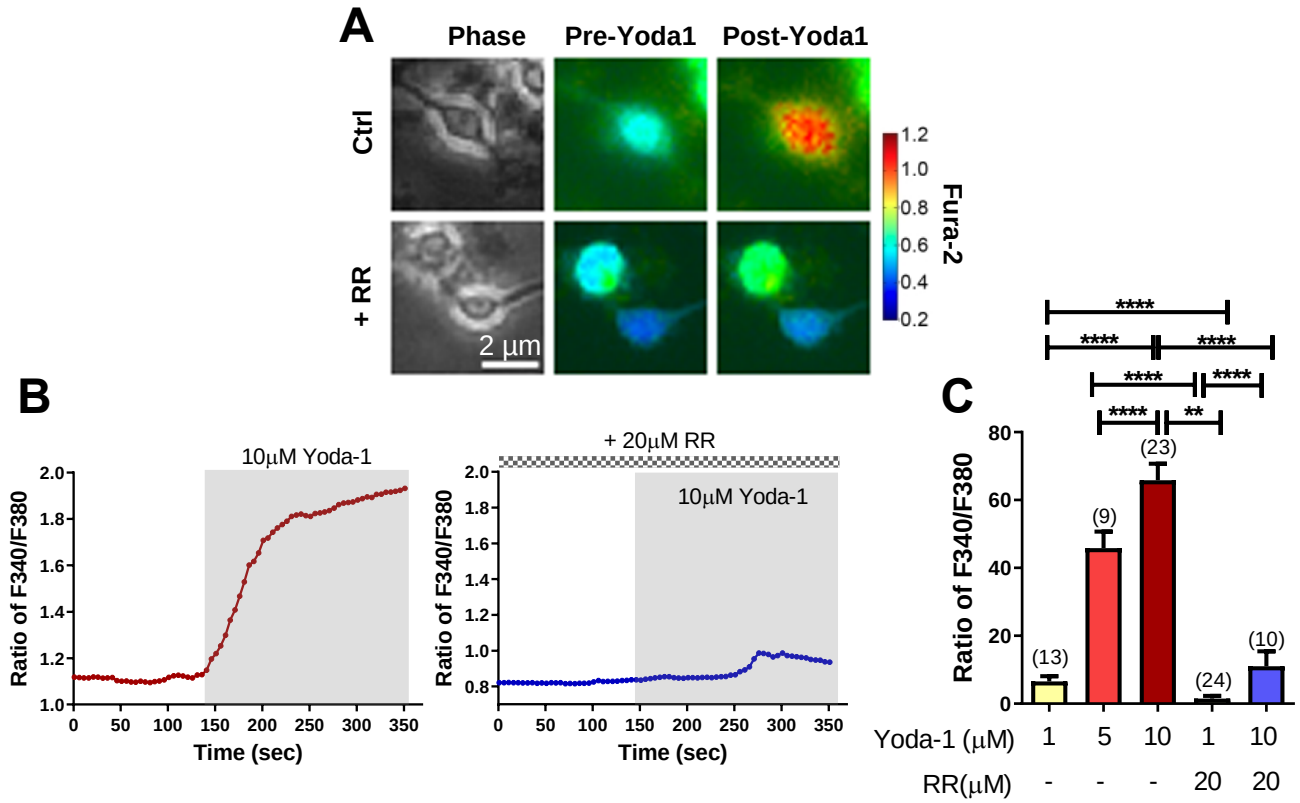

Figure S2. Detecting functional expression of Piezo1 in acutely-isolated neurons by Yoda1 stimulation, related to Figure 2

Neurons were isolated acutely from the cortices of mouse pups at P3, and treated with Piezo1 agonist Yoda1, with or without the mechanosensitive ion channel blocker Ruthenium red (RR) and imaged using the ratiometric dye Fura-2. **(A)** Representative pictures of phase contrast and Ca^{2+} imaging using the ratiometric dye Fura-2, showing the same cells prior to and after the addition of 10 µM Yoda1. **(B)** Representative Ca^{2+} imaging time-course of single neurons upon the addition of 10 µM Yoda1, with and without RR. **(C)** Quantified Ca^{2+} imaging results using Yoda1 at various concentrations, with and without the addition of RR. Bars represent mean ± SEM of 2 independent experiments. *n* for each condition is indicated above the bar; ** $P < 0.01$, **** $P < 0.0001$, unpaired one-way ANOVA with post-hoc Tukey test. All statistically-significant relationships are shown.

Transparent methods:

1. Cell culture

Human embryonic kidney (HEK) 293T cells were purchased from ATCC. CLU199 was purchased from Cedarlane Laboratories. HEK293T and CLU199 cells were maintained in Dulbecco's Modified Eagle Medium (DMEM), supplemented with 10% FBS, 10% Penicillin-Streptomycin (all from Gibco), inside a humidified incubator 37°C with 5% CO_2. For direct ultrasound treatment, cells were seeded in 35 mm culture dishes at 1 x 10^6 cells per dish, allowed to grow overnight, and treated with ultrasound the next day.

2. Plasmid transfection

The plasmid pcDNA3.1-mPiezo1-IRES-eGFP was a gift from Dr. Ardem Patapoutian (Addgene plasmid #80925; http://n2t.net/addgene:80925; RRID:Addgene_80925) and the vector control pcDNA3.1(+)IRES GFP was a gift from Kathleen L. Collins (Addgene plasmid #51406; http://n2t.net/addgene:51406; RRID:Addgene_51406). HEK293T cells were seeded into 35 mm culture dishes at 1 x 10^6 cells per dish. The next day, cells were transfected using the Lipofectamine 3000 kit (Invitrogen). 2.5 µg plasmid, 5 µl of P3000 and 5 µl of Lipofectamine 3000 were complexated in Opti-MEM medium (Gibco) according to the manufacturer's instructions and added to the cells. 24 hours later, the transfected cells were trypsinized and reseeded, partially into glass-bottomed confocal dishes (SPL Life Sciences) at 1/8 cell density, and partially back into the original dish. The cells were used for further experiments 24 hours later.

3. siRNA transfection

SMARTpool ON-TARGETplus mouse Piezo1 siRNA (L-061455-00-0005) and ON-TARGETplus Non-Targeting Pool (D-001810-10) siRNA were purchased from Dharmacon. CLU199 cells were seeded at 1 x 10^6 cells per 35 mm dish containing PLL-coated glass coverslips. Transfection complexes were prepared with Lipofectamine RNAiMAX (Invitrogen) in Opti-MEM, according to the manufacturer's instructions, such that 250 µl complexes, containing 7.5 µl Lipofectamine, were added to each plate, to a final siRNA concentration of 100 nM. Cells incubated for 48 hours before being used for further experiments.

4. Primary cortical neuron harvest

All animal procedures were approved by the Animal Subjects Ethics Sub-Committee (ASESC) of the Hong Kong Polytechnic University, and were performed in compliance with the guidelines of the Department of Health - Animals (Control of Experiments) of the Hong Kong S.A.R. government. Primary cultures of the cortices of mouse embryos at embryonic day 16 were obtained as previously described (Pi et al., 2004). Briefly, cortices were dissected in ice-cold Neurobasal medium (Gibco) and incubated in 0.25% trypsin-EDTA (Gibco) for 15 minutes. The cells were then centrifuged and washed in Neurobasal medium containing 10% FBS, 0.25% L-Glutamine and 1% Penicillin-Streptomycin (all from Gibco) and centrifuged again. The cells were resuspended in medium and gently mechanically triturated with a pipette, and then allowed to stand for 15 minutes. The resultant supernatant was discarded, and the cells were resuspended in the abovementioned medium further supplemented with 2% B27 serum-free supplement (Gibco). The cells were plated at 5 x 10^5 cells in 35 mm dishes containing poly-L-lysine-coated (PLL) coverslips, or at 1 x 10^5 cells into PLL-coated confocal dishes. After 24 hours, the medium was changed to Neurobasal + 2% B27 + 0.25% L-Glutamine + 1% Penicillin-Streptomycin. The medium was half-changed every 72 hours. Cells were used for ultrasound experiments at DIV 10.

5. Acute isolation of neurons

Neocortical pyramidal cells were isolated using a combination of enzymatic and mechanical techniques as previously described (Huguenard et al., 1989). P3 mouse pups were anaesthetized by cooling and then decapitated. Brains were quickly removed and 300 µm coronal slices containing the entire cortex were cut with a vibratome. Pieces of neocortex (1 mm^2) were trimmed, incubated in a solution of 0.25% trypsin and mechanically dispersed by trituration with pipettes. Dispersed cells were used in ratiometric calcium imaging experiments with the dye Fura-2.

6. Ultrasound stimulation system and protocol

The ultrasound stimulation system consisted of a commercial transducer (I7-0012-P-SU, Olympus), two function generators, and a power amplifier (Electronics and Innovation, A075) (as depicted in Figs 1D

and 2D) to produce 200 tone burst pulses at a center frequency of 500 kHz and a repetition frequency of 1 kHz with a duty cycle of 40%. The output intensity was limited to 0.1 - 0.5 MPa, with an interval of 10 seconds between pulses. These parameters are similar to those that have been reported to effectively evoke behavior responses (Tufail et al., 2010). Peak-to-peak pressure was measured, mapped by a customized system with a calibrated hydrophone (Onda, HGL400) held by a 3D motor. During the measurement, the transducer was tilted at 45° to the culture dish, and a hydrophone was placed on top of the culture dish. The temperature was monitored during the ultrasound treatment, and no obvious elevation was observed (data not shown).

7. Calcium imaging

Cells were loaded with the fluorescent calcium indicator Cal-590 AM (AAT Bioquest, #20510) or Fura-2 (F1200, Invitrogen), according to the manufacturer's instructions. A customized calcium imaging and ultrasound stimulation system (Figure 1D) was utilized for the study. The calcium imaging system consisted of a modified upright epifluorescence microscope. The excitation light was generated by a dual-color LED, filtered by excitation filters and delivered to the sample for illuminating the calcium sensor. The fluorescence signals from the cells were collected by a water immersion objective (UMPlanFLN, Olympus), filtered by a filter wheel with green (525 nm) or red (633 nm) channels and captured by a sCMOS camera (ORCA-Flash4.0 LT Plus C114400-42U30, Hamamatsu). To minimize phototoxic effects, the LEDs were triggered at 1 Hz and synchronized with sCMOS time-lapse imaging. To deliver ultrasound, a triangle waveguide was attached to the ultrasound transducer and placed under the culture dish at a 45-degree angle to the horizontal axis. The other site of the waveguide was mounted with an acoustic absorber to minimize acoustic reverberation. The acoustic pressure map of the system was generated using a needle hydrophone (HNR-0500, ONDA, Sunnyvale, CA, USA) and a high-precision 3D motor combined with our system. Yoda1 (Cat. No. 5586, Tocris Biosciences), a chemical agonist of Piezo1 dissolved in DMSO, was added to the cells immediately prior to imaging to a final concentration of 1 µM or 10µM. Some cells were incubated with 40 µM GsMTx-4 (Abcam, ab141871) dissolved in water, a Piezo1 incubator, in a cell culture incubator prior to calcium imaging. During calcium imaging, the cells were placed in a buffer solution with 130 mM NaCl, 2 mM $MgCl_2$, 4.5 mM KCl, 10 mM Glucose, 20 mM HEPES, and 2 mM $CaCl_2$, pH 7.4.

8. Ultrasound treatment of cells for Western blotting or c-Fos count

CLU199 cells or primary cortical neurons at DIV 10 were treated with ultrasound at acoustic pressures of 0.1, 0.3 or 0.5 MPa for 20 minutes inside a humified incubator, 37°C, 5% CO_2 using the setup depicted in Figure 2D. Some primary neurons were pre-treated with GsMTx-4 at 20 µM for 30 minutes inside an incubator, followed by the ultrasound treatment. Cells were then used for Western blotting or immunofluorescent analysis.

9. Western blotting

Cells were lysed with RIPA buffer (EMD Millipore), supplemented with 1X Halt™ Protease and Phosphatase Inhibitor Cocktail (Thermo Fisher Scientific) on ice, centrifuged to clear the lysate, and protein concentrations measured using the Bio-Rad protein assay. 30 or 50 µg total protein per well was loaded on 6% or 10% SDS-PAGE gels, electrophoresed, and transferred to nitrocellulose membranes. Membranes were blocked with 5% BSA in Tris-buffered-saline + 0.05% Tween-20 (TBST) and then incubated in primary antibody diluted in 5% BSA in TBST overnight. They were then washed with TBST and incubated in secondary antibody solutions, diluted in blocking buffer, for 1 hour at room temperature. Membranes were then washed, signals developed with SuperSignal™ West Pico or Pierce ECL (both from Thermo Scientific) chemiluminescent substrates according to the manufacturer's instructions and imaged using the Bio-Rad ChemiDoc MP system.

Primary antibodies used were phospho-CREB (#9198), phospho-CaMKII (#12716), c-Fos (#2250) all from Cell Signaling Technology and Piezo1 (15939-1-AP, Proteintech Group). c-Fos was diluted at 1:1,000 and other antibodies were diluted at 1:500. β-actin (A1978, Sigma-Aldrich) at 1: 2,000 dilution was the loading control. Secondary antibodies used were goat anti-rabbit IgG (H+L) HRP and goat anti-mouse IgG (H+L) HRP (both from Invitrogen), diluted at 1: 5,000 in blocking buffer.

Protein levels were quantified through image densitometry using ImageJ. Protein levels were expressed as a fold change compared to the untreated control, an average ± SEM of at least three

independent experiments. Statistical significance was calculated using a two-tailed unpaired student's *t*-test or one-way ANOVA as appropriate, and *P* values below 0.05 were considered significant.

10. RNA extraction and reverse-transcription

RNA was collected from cells using the GeneJET RNA Purification Kit (Thermo Scientific) according to the manufacturer's instructions, and RNA concentrations were measured using a NanoDrop One (Thermo Scientific). 1 µg RNA was reverse-transcribed using the iScript™ gDNA Clear cDNA Synthesis Kit (Bio-Rad), according to the manufacturer's instructions (including a gDNA digestion step), using a C1000 Touch thermal cycler (Bio-Rad).

11. Semi-quantitative PCR and real-time qPCR

For semi-quantitative PCR, 1 µl of first-strand cDNA product was mixed with 2X PCR Premix *Ex* Taq (Takara) (final concentration 1X), forward and reverse primers (mouse Piezo1 and β-actin, final concentration 200 nM) and H_2O to a final reaction volume of 20 µl. PCR was performed on a Bio-Rad DNA Engine thermal cyler, for 25 cycles, T_a 56°C. PCR product was loaded on a 2% agarose gel, electrophoresed, visualized in an AlphaImager HP (ProteinSimple) UV Transilluminator.

For real-time qPCR, 1 µl cDNA from plasmid-transfected HEK293T or siRNA-transfected CLU199 cells was mixed with appropriate forward and reverse primers (final concentration 250 nM), SsoAdvanced™ Universal SYBR® Green Supermix (Bio-Rad) and H_2O to a final volume of 10 µl. PCR was performed on a CFX96 Touch™ system (Bio-Rad), for 40 according to the recommended instructions of the PCR supermix manufacturer. Results are expressed as a fold change compared to the appropriate control, mean ± SEM of 3 independent experiments. Primer sequences were as follow:

Mouse β-actin: F - AGGGTGTGATGGTGGGAATG, R - TGGCGTGAGGGAGAGCATAG, 402 bp; human β-actin: F - GTGGGGCGCCCCAGGCACCA, R - CTCCTTAATGTCACGCACGATTTC, 539 bp; mouse β-actin (for qPCR): F - TATAAAACCCGGCGGCGCA, R - TCATCCATGGCGAACTGGTG, 117 bp; human β-actin (for qPCR) : F - CGGCGCCCTATAAAACCCA, R – CGCGGCGATATCATCATCCA, 142 bp; human Piezo1: F - ATCGCCATCATCTGGTTCCC, R - TGGTGAACAGCGGCTCATAG, 124 bp; mouse Piezo1: F - GCAGTGGCAGTGAGGAGATT, R - GATATGCAGGCGCCTATCCA, 143 bp.

12. Immunocytochemical fluorescent staining

Cells were fixed using 4% paraformaldehyde + PBS and permeabilized using 0.1% Triton X-100 + PBS, and all washes were done with 1X PBS. Cells were blocked using 5% normal goat serum in TBST and incubated overnight in primary antibodies diluted in 5% BSA. Secondary antibody incubation was performed the next day, diluted in 3% BSA in PBST for one hour at room temperature. Cells were washed, coverslips dried, and mounted on glass slides using small drops of Prolong Glass Antifade Mountant with NucBlue (Life Technologies) and allowed to cure overnight at room temperature. All steps from the secondary antibody incubation onwards were performed in the dark. Coverslip edges were then sealed using transparent nail enamel and imaged using a confocal laser scanning microscope (TCS SP8, Leica).

Primary antibodies used were c-Fos (Cell Signaling Technology) at a dilution of 1:5,000, Piezo1 (Proteintech Group) at a dilution of 1:200, and MAP2 (PA1-10005, Invitrogen) at a dilution of 1:1000. Secondary antibodies, used at a dilution of 1:1,000, were goat anti-rabbit IgG (H+L), Alexa Fluor 488 (A-11008) and goat anti-Chicken IgY (H+L) Alexa Fluor 633 (A-21103), all from Invitrogen.

13. c-Fos counting

The number of c-Fos$^+$ cells in primary neurons was determined by counting the number of nuclei of MAP2-expressing cells, and the number of c-Fos signals co-located with DAPI in an FOV 60 minutes after ultrasound stimulation. The percentage of nuclear c-Fos signals to the total number of neurons was calculated per experiment. Each experiment had a minimum of 10 photographed FOVs and minimum of 50 total cells counted per condition. Results from three independent experiments were averaged and subjected to a one-way ANOVA followed by a *post-hoc* Tukey test. *P* values below 0.05 were considered significant.

14. Statistical analyses

A minimum of 3 independent experiments were performed for all experiments shown. By this we mean at least 3 separate 'rounds' of cell preparations, transfections or primary neuron harvests that were

used for various experiments. Wherever possible, multiple plates from each round were evaluated. The data were collected into GraphPad Prism sheets for statistical analysis and for graph preparation. Two-tailed unpaired *t*-tests, some followed by a post-hoc Holm-Sidak correction, or one-way ANOVA with a post-hoc Tukey test were performed to determine statistical significance, were performed where appropriate. *P* values below 0.05 were considered significant.

Supplemental References

Pi, R., Li, W., Lee, N.T., Chan, H.H., Pu, Y., Chan, L.N., Sucher, N.J., Chang, D.C., Li, M., and Han, Y. (2004). Minocycline prevents glutamate-induced apoptosis of cerebellar granule neurons by differential regulation of p38 and Akt pathways. J Neurochem *91*, 1219-1230.

Huguenard, J.R., Hamill, O.P., and Prince, D.A. (1989). Sodium channels in dendrites of rat cortical pyramidal neurons. Proc Natl Acad Sci U S A *86*, 2473-2477.